Scripta Materialia 169 (2019) 28–32

Contents lists available at ScienceDirect

Scripta Materialia

journal homepage: www.elsevier.com/locate/scriptamat

The elimination of the yield point phenomenon in a new zirconium alloy: Influence of degree of recrystallization on the tensile properties

Huigang Shi [a], Jiuxiao Li [b], Jianwei Mao [a], Weijie Lu [a,*]

[a] State Key Laboratory of Metal Matrix Composites, School of Material Science and Engineering, Shanghai Jiao Tong University, Shanghai 200240, PR China
[b] School of Materials Engineering, Shanghai University of Engineering Science, Shanghai 201620, PR China

ARTICLE INFO

Article history:
Received 23 February 2018
Received in revised form 20 December 2018
Accepted 6 January 2019
Available online 13 May 2019

Keywords:
Zirconium alloys
Strain rate
Yield phenomena
Recrystallization
Dislocation mobility

ABSTRACT

The different yielding behaviors of annealed samples of Zr-Sn-Nb-Fe-Cu alloy and its dependence on microstructure have been studied. The yield drop was observed in samples with complete recrystallization, and this behavior gradually disappeared with the reduction of recrystallization degree. Meanwhile, as the strain rate increased, the yield point phenomenon (YPP) became less prominent in the stress-strain curves. It was assumed that solute-dislocation interaction mechanism and dislocation multiplication mechanism were responsible for this phenomenon. The unload-reload tests proved that the evolution of yielding behavior was caused by the increase of mobile dislocations with increasing pre-strain.

In the stress-strain curves of uniaxial tensile tests, the yield point phenomenon (YPP) shows an abrupt transition from the elastic to plastic stage, followed by a characteristic yield drop. This phenomenon has been investigated for several decades due to its industrial importance and has been widely reported in different alloys such as low carbon steels [1,2], Ti alloys [3], Al alloys [4] and Mg alloys [5]. Generally, it has been considered that both the solute-dislocation interaction mechanism [6] and dislocation-multiplication mechanism [7] are responsible for the yield drop behavior. The solute-dislocation interaction mechanism assumes that the yield drop is attributed to the tearing-off of dislocations from impurity atmospheres by the applied stress (Cottrell atmosphere) [8]. The locking of dislocations by solute atoms results in an extra stress to initiate dislocation motion. Once the dislocations break away from the Cottrell atmosphere, a steep decrease in stress is observed. On the other hand, the dislocation-multiplication mechanism considers that the yield drop is due to the lack of mobile dislocations in materials [9]. The rapid proliferation of dislocations at the early stage of slip deformation allows the dislocations to move more slowly because the strain rate is proportional to both the mobile dislocation density and the dislocation velocity, then leading to a yield drop after dislocation motion has been initiated.

Zirconium alloys are of considerable technological importance in the nuclear industry as structural materials and as cladding for nuclear fuel in fuel assemblies [10]. The YPP in zirconium alloys has been investigated by some researchers. Veevers [11] concluded that a dislocation cell structure was the precondition for the yield drop to occur and the pinning of dislocations by oxygen interstitial atoms was responsible for the YPP in Zircaloy-2. Thorpe [12] believed that the dislocation locking was attributed to a Snoek ordering mechanism [13], which was responsible for the yield drop in Zr-1 wt% Nb alloy. This was thought to occur by the stress-induced diffusion of interstitial oxygen atoms in the neighbourhood of substitutional atoms.

Recently, we found that a new Zr-based alloy exhibited YPP during tension tests at room temperature and the yield drop could be explained by the dislocation-multiplication mechanism [14], which was inconsistent with previous studies. In an attempt to shed further light on the mechanism of YPP in zirconium alloys, a study of the effect of recrystallization degree on the yielding characteristics was undertaken. The Zr-Sn-Nb-Fe-Cu alloy was prepared by three kinds of heat treatment to obtain different microstructures, and the tensile properties of the experimental alloys were characterized by uniaxial tensile tests.

The detailed composition of the material was Zr-0.49Sn-0.43Nb-0.28Fe-0.047Cu (wt%). The as-received samples were prepared by a sequence of three times vacuum arc re-melting, a hot forging at 1000 °C, a β-quenching at 1050 °C, a hot rolling at 600 °C and four times of cold rolling. Then samples were divided into three groups by different heat treatments: (a) annealed at 550 °C/5 h; (b) annealed at 500 °C/5 h; (c) β-quenched and annealed at 480 °C/5 h.

Dog-bone flat tensile specimens with nominal gauge section of 20 × 12 × 0.6 mm (L × W × H) were cut from in the rolling direction

* Corresponding author: State Key Laboratory of Metal Matrix Composites, School of Material Science and Engineering, Shanghai Jiao Tong University, Shanghai 200240, PR China.
E-mail address: luweijie@sjtu.edu.cn (W. Lu).

https://doi.org/10.1016/j.scriptamat.2019.05.008
1359-6462/

(RD). Room temperature tension tests were performed at strain rates of 1×10^{-4} to 1×10^{-1} s^{-1} using a Zwick Z100/SN3A universal testing machine.

The microstructures of the annealed specimens were characterized by electron back-scatter diffraction (EBSD) analysis system (Channel 5, AZtec HKL Max), installed on a Mira 3 scanning electron microscope.

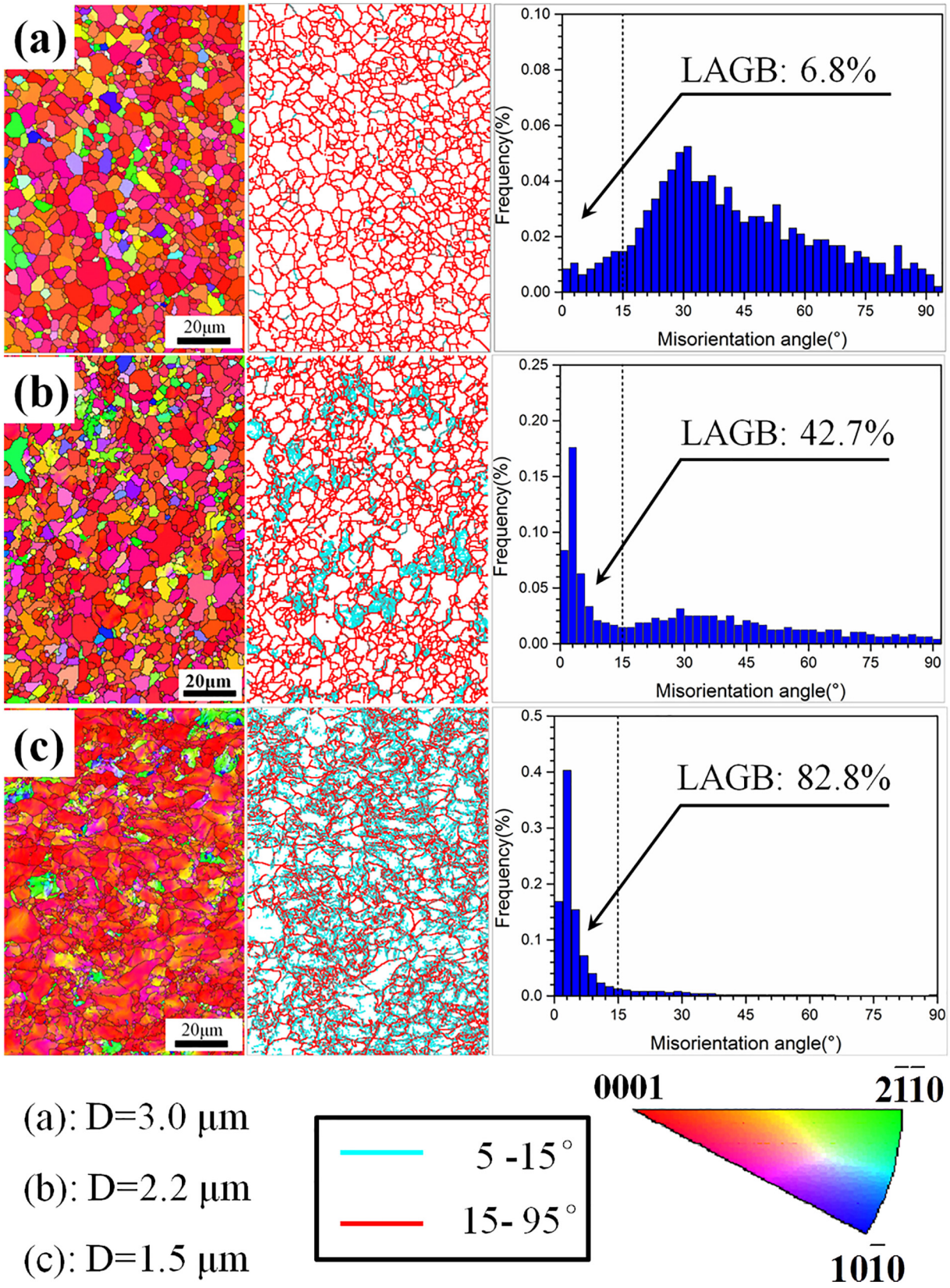

Fig. 1. EBSD inverse pole figure (IPF) map, grain boundary (GB) map and mis-orientation angle distribution (MAD) in the samples for (a) 550 °C/5 h; (b) 500 °C/5 h and (c) β-quenched and 480 °C/5 h, respectively.

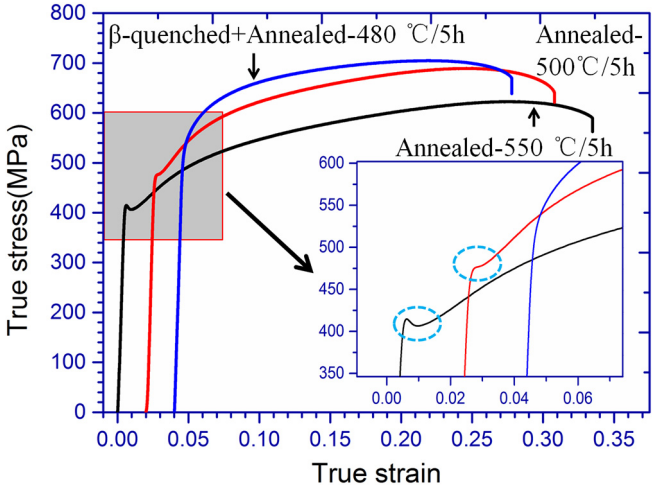

Fig. 2. True stress-strain curves under the quasi-static tension tests for the three samples at room temperature. The inset demonstrates the initial yielding behaviors for three alloys.

EBSD data for each sample were collected at step size of 0.1 μm with a scanning area of 90 × 130 μm^2 on the surface determined by rolling direction (RD) and normal direction (ND).

Fig. 1 displays the inverse pole figure (IPF) maps, grain boundary (GB) maps and mis-orientation angle distribution (MAD) histograms derived from EBSD data for the three alloys. As shown in the IPF maps, the sample is composed of well-equiaxed grains after 550 °C/5 h treatment, indicative of a fully recrystallization microstructure (denoted as F-Rec sample). Nevertheless, apart from the well-equiaxed grains, many fine grains (<0.5 μm) are observed in the sample after 500 °C/5 h annealing. Meanwhile, the orientations (colors) of some grains are not uniform according to the standard triangle at the bottom of Fig. 1. It is assumed that these non-uniform grains are the remnant products by the cold rolling, indicating that partial recrystallized microstructure is obtained after 550 °C/5 h treatment (denoted as P-Rec sample). After β-quenched and 480 °C/5 h heat treatment, the sample is dominated by irregular grains, surrounding by lots of fine grains. The irregular grains usually have long strip structures, with non-uniform orientations, implying that the sample is still at the initial stage of recrystallization (denoted as N-Rec sample). Besides, the mean grain size increased with increasing annealed temperature. With respect to GB maps, it is clear that high angle grain boundaries (HAGBs, marked as red line) are predominant over low angle grain boundaries (LAGBs, marked as sky-blue line) for F-Rec sample. Nearly half of GBs possess LAGBs for P-Rec sample, and large amount of LAGBs are dominant in the GB maps for N-Rec sample. Thus, it can be concluded that the proportion of LAGBs increased with the decrease of annealing temperature. This trend can also be seen in their MAD histograms by a quantitative measurement. As is seen, the fraction of LAGBs gradually increased from 6.8% to 82.8% with the decrement of annealing temperature. In the annealing process, the sub-grains will coalesce together by grain boundaries migration and dislocation slip, leading to the recrystallization nucleation behavior. These sub-grains continue to grow up towards the deformed grains, and LAGBs are gradually transformed to HAGBs. The higher the annealing temperature, the higher the recrystallization degree.

Fig. 2 presents the true stress-strain curves in the tension tests with strain rate of 10^{-3} s^{-1} for the three specimens. As is seen, the elongation increases with increasing annealing temperature, whereas the yield strength decreases with increasing annealing temperature. It is worth noting that a clear yield drop at the initial stage of yielding is observed for F-Rec sample, whereas a yield plateau is obtained for P-Rec sample

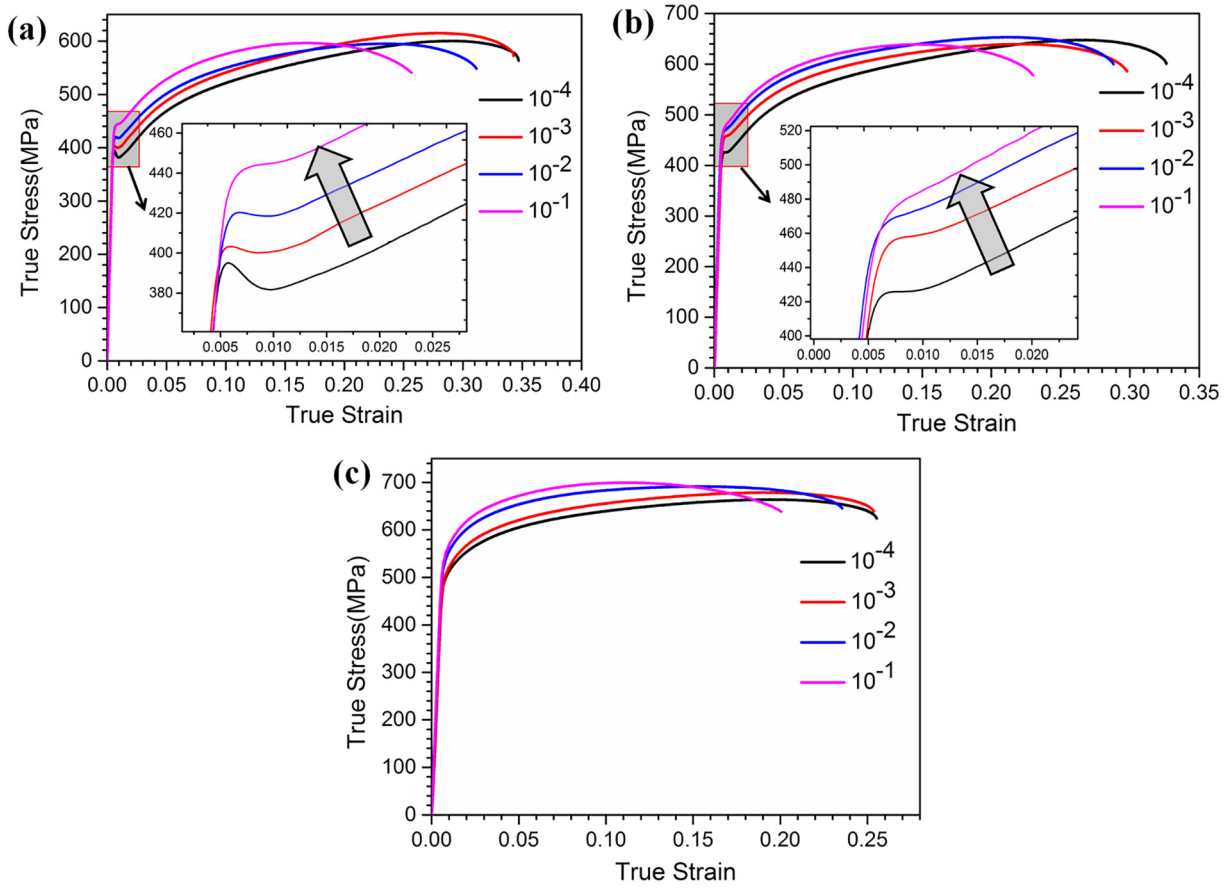

Fig. 3. Effect of strain rate on the tensile properties of the three samples: (a) F-Rec sample; (b) P-Rec sample; (c) N-Rec sample.

(sky-blue circles in the inset figure). This discontinuous yielding is eliminated for N-Rec sample with no infection in stress-strain curve. Therefore, it can be concluded that the YPP gradually disappears at the early stage of deformation with decreasing recrystallization degree of alloys.

Fig. 3 shows the effect of strain rate $\dot{\varepsilon}$ on the tensile properties of the three samples tested at room temperature. As $\dot{\varepsilon}$ increases, the flow stress increases monotonically and the tensile ductility tends to decrease in all samples. It is noteworthy that the extent of the yield drop becomes less prominent with increasing $\dot{\varepsilon}$ in F-Rec specimen (Fig. 3a), and the yield plateau gradually vanishes with increasing $\dot{\varepsilon}$ in P-Rec sample (Fig. 3b).

It is well known that dislocations can be locked by solute atoms to form Cottrell atmosphere [8] or Snoek atmosphere [15]. Once the dislocations break away from solute atmosphere, the stress required for dislocation motion decreases. Previous studies [12] suggested that Snoek ordering of atom pairs was responsible for the yield drop after aging in Zr-Nb alloy. Therefore, it is likely possible that local atomic rearrangement or short-range ordering may take place in the stress field of some moving dislocations, leading to a dragging effect to some mobile dislocations in our materials.

On the other hand, the classic work by Johnston and Gilman [16] proposed that yield drop was due to the lack of mobile dislocations and rapid multiplication of mobile dislocations at the initial stage of slip deformation. It is well known that the LAGBs can be seen as a series of edge dislocations, screw dislocations or mixed dislocations, which are arranged parallel or entangled with each other. In F-Rec sample, due to the extremely low fraction of LAGBs (6.8%), the mobile dislocation density ρ_m accumulated in the LAGBs is low and can be estimated by the expression [17]:

$$\rho_m = \frac{3\overline{\theta}_{LAGB} f_{LAGB}}{bD} \tag{1}$$

where $\overline{\theta}_{LAGB}$ is the average boundary mis-orientation angle of LAGBs; f_{LAGBs} is the fraction of LAGBs; b is the magnitude of the Burgers vector of dislocations and D is the average grain size. According to the Orowan equation, the internal shear strain rate $\dot{\gamma}$ can be expressed by

$$\dot{\gamma} = b\rho_m v \tag{2}$$

and

$$v = \left({}^{\tau}/_{\tau_0}\right)^n \tag{3}$$

in which v is the average velocity of dislocations, τ_0 is the stress required for dislocation to move at unit velocity, τ is the effective shear stress acting on the dislocation and n is the stress sensitivity index. Using the relationship between tensile and shear strain rate as $\dot{\varepsilon} = \dot{\gamma}/M$ (where M is the Taylor factor) and combining Eqs. (1)–(3), we can write:

$$\tau = \sqrt[n]{\frac{\dot{\varepsilon} MD}{3\overline{\theta}_{LAGB} f_{LAGB}}} \cdot \tau_0 \tag{4}$$

Eq. (4) confirms that shear stress τ is inversely proportional to the fraction of LAGBs f_{LAGB}. To maintain the constant value of $\dot{\varepsilon}$ during the tensile tests, the value of τ must be high (upper yield point) due to the low value of f_{LAGB}. Once the plastic deformation begins, the dislocations proliferate rapidly and the shear stress drops abruptly (lower yield point).

In P-Rec sample, the fraction of LAGBs is 42.7%. At the onset of slip deformation, the shear stress (upper yield point) is not high according to Eq. (4). After yielding, the mobile dislocation density varies little because the pre-stored mobile dislocations can be activated at the beginning of tensile loading, result in a minor change on the shear stress (lower yield point). Thus, a yield plateau occurs at the initial stage of yielding. In contrast, the initial density of mobile dislocations increases in N-Rec sample. The high density of mobile dislocations results in the easy gliding of themselves and contributes to the disappearance of YPP. Furthermore, the extra mobile dislocations interact with grain boundaries and a direct work hardening occurs with no inflection in the stress-strain curves.

The strain rate dependence of the yielding behavior can be explained in terms of the Cottrell-Bilby theory [18]. At low strain rates the solute atmospheres can diffuse with the dislocations, but at high strain rates the dislocations will escape from their atmospheres, and multiply. Thus, the initial mobile dislocations in the materials increases as the strain rate increases, leading to the decrease of yield drop and the gradual disappearance of YPP.

In order to verify our inference, unloading-reloading tensile tests with different pre-strains were conducted for F-Rec sample. As shown in Fig. 4, the YPP gradually fades away with the increase of pre-strain. When the pre-strain $\varepsilon = 0.5\%$, the re-loaded curve shows a relatively lower yield drop compared with no pre-strained curve. As the pre-strain increases to 0.7%, a yield plateau is observed in the re-loaded curve. With the further increase of pre-strain to 1% and 3%, there is a direct work hardening at the initial stage of reloaded curves, and the

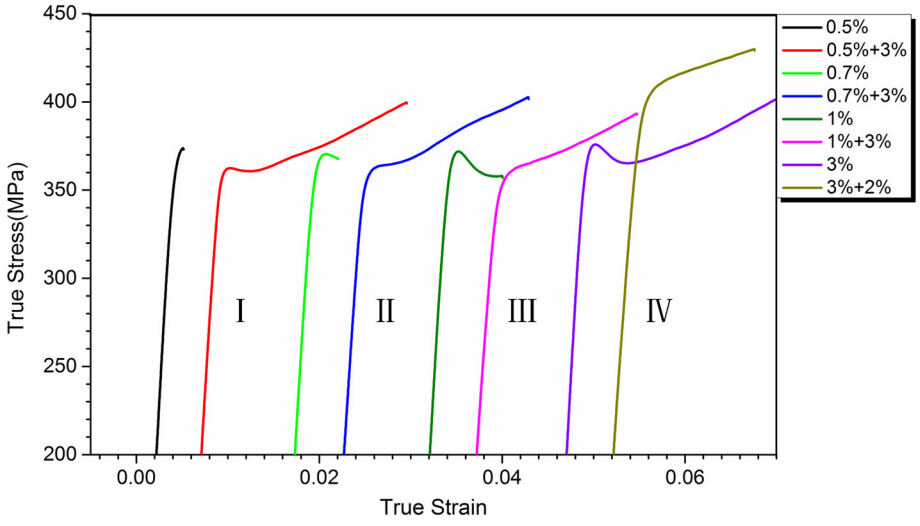

Fig. 4. Unloading-reloading stress-strain curves for F-Rec sample with different pre-strains (I) 0.5%; (II) 0.7%; (III) 1%; (IV) 3%.

larger the pre-strain, the higher the yield strength. It is believed that mobile dislocations will be introduced by the pre-strain deformation, and the mobile dislocations increased with increasing pre-strain. Accordingly, the yield drop dwindles and the YPP gradually disappears with the increase of pre-existed mobile dislocations.

In summary, the effects of recrystallization degree on the yielding behaviors at room temperature of Zr-Sn-Nb-Fe-Cu alloys were investigated. It was demonstrated that a yield drop was obtained in samples with fully recrystallized microstructure, while a yield plateau was observed in the partially recrystallized specimens, and the direct work hardening with no inflection was found in samples which were at the initial stage of recrystallization. The gradual absence of yield drop phenomenon with the decrease of recrystallization degree was interpreted in terms of solute-dislocation interaction and dislocation multiplication mechanism. The effect of strain rate on the tensile properties was investigated and the extent of yield drop became weaker with increasing strain rate, which was attributed to the dislocations breaking away from the impurity atmosphere. The unloading-reloading tension tests with different pre-strains reproduced the evolution of yielding behaviors from yield drop to work hardening with the increase of pre-strain.

The present study was financially supported by the National Natural Science Foundation of China (Grant No: U1602274, 51741108, 51371114, 51875349, 51501112), the 111 Project (Grant No. B16032) and the Laboratory Innovative Research Program of Shanghai Jiao Tong University (Grant No. 17SJ-14).

References

[1] N. Tsuchida, H. Masuda, Y. Harada, K. Fukaura, Y. Tomota, K. Nagai, Mater. Sci. Eng. A 488 (2008) 446–452.
[2] D. Akama, N. Nakada, T. Tsuchiyama, S. Takaki, A. Hironaka, Scr. Mater. 82 (2014) 13–16.
[3] S.M. Abbasi, M. Morakabati, A.H. Sheikhali, A. Momeni, Metall. Mater. Trans. A 45A (2014) 5201–5211.
[4] C.Y. Yu, P.W. Kao, C.P. Chang, Acta Mater. 53 (2005) 4019–4028.
[5] M.R. Barnett, M.D. Nave, A. Ghaderi, Acta Mater. 60 (2010) 1433–1443.
[6] R. Schwab, V. Ruff, Acta Mater. 61 (2013) 1798–1808.
[7] J.P. Hirth, J. Lothe, Theory of Dislocations, John Wiley and Sons, New York, 1982.
[8] A.H. Cottrell, B.A. Bilby, Proc. Phys. Soc. London, Sect. A 62 (1949) 49–62.
[9] E.O. Hall, Yield Point Phenomenon in Metals and Alloys, Plenum Press, New York, 1970 65.
[10] A.T. Motta, A. Couet, R.J. Comstock, Annu. Rev. Mater. Res. 45 (2015) 311–343.
[11] K. Veevers, K.U. Snowden, J. Nucl. Mater. 47 (1973) 311–316.
[12] W.R. Thorpe, I.O. Smith, J. Nucl. Mater. 80 (1979) 35–42.
[13] J.T. Evans, R.M. Douthwaite, Acta Metall. 21 (1973) 49–54.
[14] H.G. Shi, X.L. Guo, J.X. Li, J.W. Mao, J.Q. Lu, W.J. Lu, Mater. Charact. 151 (2019) 84–95.
[15] F.X. Jiang, T.Y. Zhang, Scr. Metall. 22 (1988) 773–777.
[16] W.G. Johnston, J.J. Gilman, J. Appl. Phys. 30 (1959) 129.
[17] D.A. Hughes, N. Hansen, Acta Mater. 48 (2000) 2985–3004.
[18] A.H. Cottrell, D.L. Dexter, Dislocations and Plastic Flow in Crystals, Clarendon Press, Oxford, 1956.